JOURNAL OF MAGNETIC RESONANCE **133,** 61–69 (1998)
ARTICLE NO. MN981432

# Resolution Enhancement in Multiple-Quantum MAS NMR Spectroscopy

Ingo Schnell, Adonis Lupulescu, Siegfried Hafner, Dan E. Demco, and Hans W. Spiess[1]

*Max-Planck-Institut für Polymerforschung, Postfach 3148, D-55021 Mainz, Germany*

Received November 13, 1997

**Two techniques for resolution and sensitivity enhancement are introduced in multiple-quantum (MQ) MAS spectroscopy of rigid solids. The first makes use of ultrafast MAS with spinning frequencies of up to 35 kHz, while the second combines MAS at moderately fast spinning frequencies of about 13 kHz with multiple-pulse (MP) dipolar decoupling. For the latter approach, a semiwindowless WHH-4 sequence is applied during the MQ evolution period (MQ dimension) and/or detection period (single-quantum dimension). In the MQ dimension, the MP sequence has to be supplemented by two bracketing pulses in order to preserve the order and the intensities of the evolving MQ coherences. Double-quantum $^1$H NMR spectra of L-alanine recorded using both decoupling techniques are shown and compared to each other. Triple-quantum $^1$H NMR spectra under ultrafast MAS conditions are also presented.** 

## INTRODUCTION

In the past years, the field of solid-state multiple-quantum (MQ) NMR spectroscopy (*1, 2*) has developed into an important tool for characterizing materials on molecular length scales. In order to resolve chemically distinct sites by averaging of the anisotropic spin interactions also in solids, MQ spectroscopy has been combined with magic-angle spinning (MAS). Such high-resolution MQ MAS techniques were introduced for dipolar-coupled homonuclear $^1$H (*3–9*), $^{31}$P (*10–13*), $^{13}$C (*14*), and heteronuclear $^1$H–$^{13}$C (*15–17*) spin-$\frac{1}{2}$ systems as well as for half-integer quadrupolar nuclei (*18–24*, and references therein). Applying these techniques, internuclear distances, residual dipolar couplings, and quadrupolar coupling parameters could be measured.

For high-resolution MQ experiments in rigid spin-$\frac{1}{2}$ systems, the handling of the dipolar interaction is particularly challenging because of its complexity and the homogenous nature of the resulting line broadening. On one hand, the dependence of this interaction on internuclear distances and molecular orientations can be exploited to extract information on both structure and dynamics. First, 2D MQ MAS spectra provide directly qualitative insight into dipolar connectivities. In addition to that, analyzing MQ buildup intensities and MQ spinning sideband patterns of various order provides quantitative information on the strength of dipolar couplings (*4, 14*) and the topology of the spin system can be obtained (*8*). On the other hand, it has been shown (*8*) that for extended dipolar-coupled networks the remaining dipolar broadening of resonance lines in spinning-sideband patterns leads to a severe loss in spectral resolution. Moreover, the structural and dynamic information is difficult to extract from complex many-spin topologies. Hence, an efficient dipolar decoupling technique is desirable, which provides sufficient spectral resolution and simplifies the network of spin–spin interactions to such an extent that it can be handled for extracting detailed information.

In the MQ investigations performed to date, the decoupling of the homonuclear dipolar interaction was based solely on MAS with the routinely available spinning frequencies of up to 15 kHz. The advantage of technical simplicity is accompanied by the limited line-narrowing efficiency, in particular when MAS is applied to rigid solids with a static $^1$H linewidth of 50 kHz and more. The investigations of this paper, therefore, aim to improve the resolution in solid-state MQ spectroscopy by introducing ultrafast MAS with a spinning frequency of 35 kHz and, alternatively, multiple-pulse (MP) assisted MAS (*25–27*). The efficiencies of the different approaches are compared.

## METHOD

### *Excitation of Multiple-Quantum Coherences*

The general schematic representation of an MQ MAS experiment is shown in Fig. 1a. During the excitation period, MQ coherences between dipolar-coupled spins are generated by the action of an effective Hamiltonian $H_{exc}$, producing a density operator of the form

$$\rho(\tau_{exc}) = \exp\{-iH_{exc}\tau_{exc}\}\rho(0)\exp\{+iH_{exc}\tau_{exc}\}. \quad [1]$$

$\tau_{exc}$ is the excitation time, and $\rho(0)$ the initial density operator which is, when starting with $z$-polarization and setting the factor of proportionality to unity, equal to $I_z$.

Depending on the effective dipolar coupling strength, the excitation of MQ coherences can follow two strategies: first, short-time excitation with $\tau_{exc} \leq \tau_R/2$, such that the dipolar

[1] To whom correspondence should be addressed.



1090-7807/98 $25.00

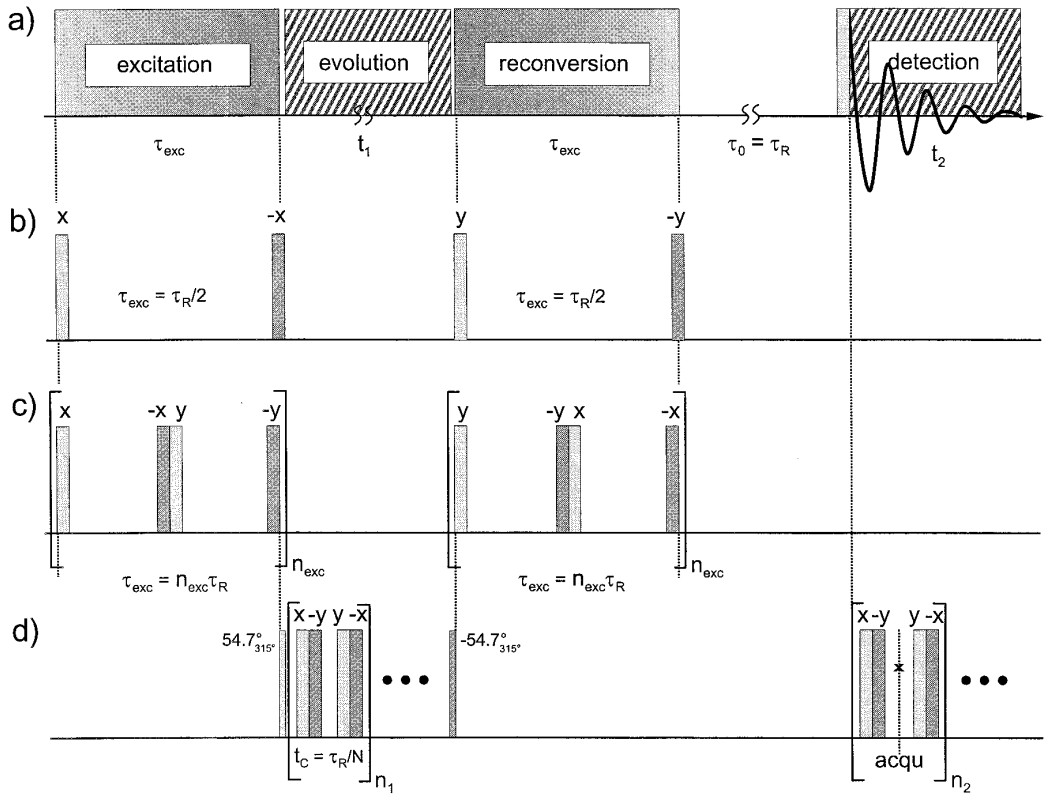


**FIG. 1.** (a) Schematic representation of a two-dimensional MQ experiment. In both spectral dimensions (MQ coherences in $t_1$ and SQ coherences in $t_2$), dipolar decoupling can be achieved either by MAS only or by MAS combined with MP techniques. (b) Five-pulse sequence used for the excitation of MQ coherences under MAS at $\omega_R/2\pi = 13$ kHz. The timing $\tau_{exc} = \tau_R/2$ avoids phase distortions and gives rise to characteristic spinning sideband patterns in the resulting MQ MAS spectrum (*8, 41*). (c) BABA recoupling pulse sequence used for the excitation of MQ coherences under MAS at $\omega_R/2\pi = 35$ kHz. For $^1$H DQ excitation in L-alanine, the excitation period was set equal to $\tau_{exc} = \tau_R$, whereas TQ coherences were excited with $\tau_{exc} = 2\tau_R$, additionally applying two bracketing 90° pulses with $y$ and $-y$ phase at the beginning of the excitation period and at the end of the reconversion period, respectively. (d) Pulse sequences consisting of WHH-4 cycles used for dipolar decoupling during MQ evolution $t_1$ and detection $t_2$, respectively. For $t_1$-decoupling, the WHH-4 cycles are rotor synchronized and bracketing 54.7° pulses are applied in the [1,1̄,0]-direction, that is, with a phase of 315°. These bracketing pulses flip the magnetization onto the effective precession axis, in order to preserve the order of evolving MQ coherences. During $t_2$, the WHH-4 cycle is not fully synchronized, following the direct detection technique described in Ref. (*26*).

interaction is only partially averaged by MAS; and second, recoupling techniques with $\tau_{exc} = n \cdot \tau_R$, in which the pulse sequence compensates the dipolar decoupling of MAS (*28*). In this paper, for rigid proton systems and moderate spinning frequencies $\omega_R/2\pi \approx 13$ kHz, short-time excitation was applied using the five-pulse sequence (*1, 4, 8*) of Fig. 1b with $\tau_{exc} = \tau_R/2$. The timing is chosen such that, in the MQ spectrum, phase distortions are avoided and characteristic double-quantum (DQ) and triple-quantum (TQ) MAS patterns are excited for spin pairs and methyl-like systems, respectively (*8*). For spinning frequencies $\omega_R/2\pi \approx 35$ kHz, the BABA recoupling sequence (*10, 14*) of Fig. 1c was applied.

Both pulse sequences in Figs. 1b and 1c excite MQ coherences of only even order, whereas odd-order MQ coherences are generated either by a five-pulse sequence of the form $90^\circ_\varphi$–$\tau_{exc}$–$90^\circ_{\varphi+\pi/2}$–$t_1$–$90^\circ_{\varphi+\pi/2}$–$\tau_{exc}$–$90^\circ_\varphi$–$\tau_0$–$90^\circ_{\varphi'}$–$t_2$ acting on $\rho(0) \propto I_z$ (*8*), or by application of recoupling pulse sequences on $\rho(0) \propto I_{x,y}$ spin modes which are generated by two bracketing 90° pulses, one before the excitation and one after the reconversion period.

The excited MQ coherences can be expressed (*1*) in terms of irreducible tensor operators $T_{l,m}$ of rank $l$ and order $m$, that is,

$$\rho(\tau_{exc}) = \sum_{k,l,m} b^{(k)}_{l,m} T^{(k)}_{l,m}, \qquad [2]$$

where the quantum number $m$ can be identified with the coherence order, and $b^{(k)}_{l,m}$ are Liouville-space coordinates. The index $k$ distinguishes different operators with the same transformation properties.

### *Conservation of the MQ Coherence Order in $t_1$*

After the excitation, the MQ coherences evolve under the resonance offset, the chemical-shielding interactions, and the dipolar coupling to spins which are not involved in the considered MQ coherence. The isotropic chemical shift provides

the desired spectral resolution of the chemically distinct sites, whereas the dipolar interaction broadens the MQ resonance lines increasingly with the order of the selected MQ coherence, as has recently been shown for TQ MAS spectra (*8*). To improve resolution, it is therefore essential to reduce this undesired broadening in the evolution and/or detection period. During excitation and reconversion, however, the dipolar interaction has to be retained or even to be recoupled.

During the evolution period, care must be taken to preserve the order of the excited MQ coherences. Unlike for MAS, this is not automatically guaranteed when applying MP sequences for dipolar decoupling. This is because the total average Hamiltonian includes contributions of off-resonance and chemical-shielding interactions. In the toggling-frame representation, we can write for this contribution

$$\bar{H}^{(0)} = k \sum_i (\delta_i + \Delta\omega)(c_x I_x^{(i)} + c_y I_y^{(i)} + c_z I_z^{(i)}), \qquad [3]$$

where $k$ is a numerical factor related to the scaling factor $S$ of the MP dipolar decoupling sequence. $\delta_i$ is the isotropic chemical shift of the spins $i$, and $\Delta\omega$ is the off-resonance frequency. $\vec{I}^{(i)}$ denotes the total spin operator of the nucleus $i$, and the $c_\alpha$ ($\alpha = x, y, z$) are Cartesian spin-operator coordinates which depend on the applied MP sequence (*29, 30*).

Consider the short-time evolution of MQ coherences, that is, using the Liouville formalism,

$$\exp(-i\hat{\bar{H}}^{(0)}t_c) \cdot T_{l,m}^{(k)} \approx T_{l,m}^{(k)} - i\hat{\bar{H}}^{(0)} T_{l,m}^{(k)} t_c + \frac{1}{2}\hat{\bar{H}}^{(0)}\hat{\bar{H}}^{(0)} T_{l,m}^{(k)} t_c^2 + \ldots, \qquad [4]$$

where $t_c$ is the cycle time of the MP sequence, and the Liouville operator $\hat{\bar{H}}^{(0)}$ corresponds to Eq. [3]. Since $\hat{\bar{H}}^{(0)}$ contains $I_x$ and $I_y$ spin operators, and $[T_{l,m}^{(k)}, T_{1,\pm1}^{(k)}] \neq 0$, where $T_{l,m}^{(k)}$ represents MQ coherences of order $m$, involving nucleus $k$, and $T_{1,\pm1}^{(k)} = \mp 1/\sqrt{2}(I_x^{(k)} \pm I_y^{(k)})$, the MQ coherences are not retained. In fact, $\bar{H}^{(0)}$ describes rotations which change the order $m$ (but not the rank $l$) of the irreducible-tensor operators (*1*). Therefore, coherences of different orders are generated from the originally excited coherences. This process results in a damping of the original coherences with time, which causes line broadening and hence a loss in spectral resolution. Moreover, there is experimental evidence that these new coherences generated by $\hat{\bar{H}}^{(0)}$ give rise to additional signals, since they retain a finite phase memory and, therefore, pass the phase-cycling procedure used for MQ-order selection. These signals overlap with the MQ spectrum of the desired order. Thus, conversion of the MQ order during the evolution period also vitiates the quantitative interpretation of the MQ spectrum.

The conversion effect can be cured by application of additional pulses, such that the evolution can be described in a tilted rotating frame with axes ($X, Y, Z$), in which the average Hamiltonian is $\tilde{\bar{H}}^{(0)} \propto I_z$. This can be achieved by bracketing the MP sequence with two phase-alternated sandwich pulses (*31*) as outlined later in more detail for a particular sequence.

Moreover, when discussing the conservation of the MQ coherence order during the action of the average (chemical shift and dipolar) Hamiltonian $\bar{H}$ of a MP decoupling sequence, the effect of higher-order terms of the Magnus expansion for times $t = n \cdot t_c$ (*29, 30*) has also to be taken into account, that is,

$$\bar{H} = \bar{H}^{(0)} + \bar{H}^{(1)} + \bar{H}^{(2)} + \ldots. \qquad [5]$$

The higher-order terms continuously change the spin-correlation order and the order of the evolving MQ coherences, the first reflected in the rank $l$ of the tensor operators $T_{l,m}$, the latter in the order $m$ (cf. Eq. [4]). These changes also result in line broadening and the presence of additional MQ orders. In MP line-narrowing experiments, these effects of higher-order terms are usually dealt with by confining to short cycle times and by high-order compensating sequences. Under the conditions of fast sample spinning, as investigated here, higher-order compensation is left to MAS (*25, 26*).

### *Dipolar Decoupling of the MQ Evolution*

In order to average dipolar couplings during the evolution period, two strategies are possible (*32*). The most straightforward technique is to increase the MAS frequency to the ultimately possible value, which presently is around 35 kHz. The advantage of this pure MAS approach is that there are no artifacts generated by radio-frequency (RF) pulse imperfections, since MAS modulates solely the space part of the interactions.

An alternative line-narrowing technique is the application of MP sequences at moderately fast MAS frequencies. It is well known that MP line narrowing and MAS might interfere with each other when applied on about the same time scale. In order to avoid such an interference, both techniques can be either appropriately synchronized (*27*) or performed on different time scales. In the latter case, the faster one (usually MP) is applied under quasi-static conditions. Conventional CRAMPS experiments use this approach by confining to MAS frequencies of around 3 kHz (*33–35*).

It has recently been shown (*25, 26*) that similar experiments can also be performed at MAS frequencies of up to 15 kHz by decreasing the length of the pulse cycle as much as possible and complying with the synchronization conditions. This can be accomplished by use of windowless or semiwindowless MP sequences which consist only of a short basic cycle. As a consequence of that design, the MP sequence does not compensate effects of high-order terms (cf. Eq. [5]) and cannot be supposed to remove the dipolar interaction completely. In such experiments, the MP technique is meant to reduce the dipolar interaction to such an extent that, in a second averaging process, the residual parts can be dealt with by fast MAS, which

also removes the effects of other imperfections of the MP experiment and further anisotropic interactions. In comparison to conventional CRAMPS experiments, this additional fast-MAS averaging process makes the *multiple-pulse assisted MAS* approach much more forgiving with respect to hardware limitations and misadjustments. It is therefore particularly suitable for application within a 2D experiment.

Following this approach, the semiwindowless WHH-4 sequence (*29, 30*) was applied during the evolution period of the MQ experiment (see Fig. 1d). As already outlined, care has to be taken that the selected MQ coherences do not change their order during the $t_1$ evolution, since for most MP sequences the off-resonance and chemical-shift evolution takes place around an axis different from $I_z$. For the WHH-4 sequence, for example, the off-resonance and chemical-shift Hamiltonians in the toggling frame are $\bar{H}^{WHH}_{off,CS} \propto \frac{1}{3}(I_x + I_y + I_z)$ (*29, 30*) and, therefore, convert the orders of MQ coherences. In order to prevent this, the respective Hamiltonian has to be transformed such that

$$\tilde{H}^{WHH}_{off,CS} = -S(\delta + \Delta\omega)I_z, \qquad [6]$$

where only one spin species was considered for simplicity (cf. Eq. [3]). The effect of $\tilde{H}^{WHH}_{off,CS}$ on the MQ coherences represented by $T^{(k)}_{l,m}$ is then given by

$$\exp(-iS(\delta + \Delta\omega)I_z t) \cdot T^{(k)}_{l,m} \cdot \exp(iS(\delta + \Delta\omega)I_z t) = \exp(-iS(\delta + \Delta\omega)mt)T^{(k)}_{l,m}. \qquad [7]$$

Thus, the only effect is a scaling of the frequency by a factor $S(\delta + \Delta\omega)m$, where $S$ is the scaling factor of the decoupling MP sequence.

For the WHH-4 sequence, the necessary transformation is performed by bracketing the MP train by two pulses with flip angles $\theta_m = \pm 54.74°$ oriented along the $[1,\bar{1},0]$-direction in the rotating frame (*31*), that is, a pulse phase of 315° (see Fig. 1d). In the spin space, the action of this pulse can be decomposed in a cascade of three rotations:

$$\exp(-i\,\tfrac{\pi}{4}\,\hat{I}_z)\exp(-i\theta_m\hat{I}_{x'})\exp(i\,\tfrac{\pi}{4}\,\hat{I}_z) \times \{\tfrac{1}{3}\,(I_x + I_y + I_z)\} = 1/\sqrt{3}\; I_z, \qquad [8]$$

where, by spin rotations (written as Liouville operators), we pass through various reference frames: $(x, y, z) \rightarrow (x', y', z') \rightarrow (X,Y,Z)$. The resulting scaling factor is $S = 1/\sqrt{3} \cong 0.58$. For simplicity, this treatment was performed in the $\delta$-pulse limit, which means that the coordinates $c_\alpha$ in Eq. [3] are assumed to be the same for all $\alpha = x, y, z$. For the experimentally applied semiwindowless variant of the WHH-4 sequence, the actual coefficients in Eq. [3] are $c_x = c_z = 1.138$ and $c_y = 1.273$, which results in a scaling factor $S \cong 0.554$. This minor difference between both cases can be neglected in the limits of the experimental accuracy.

In the preceding treatment, the bracketing pulses are supposed to act on the Hamiltonians. An equivalent approach is to consider them as preparation pulses which align the initial state $\rho(\tau_{exc})$ orthogonal to the effective Hamiltonian $\bar{H}^{WHH}_{off,CS}$ acting in $t_1$. This strategy is well known from conventional single-quantum (SQ) decoupling experiments where a corresponding preparation pulse is usually applied to maximize the contribution of the signal which is encoded by the chemical shift. In the case of MQ coherences, however, these bracketing pulses are also essential for preserving the order of the observed MQ coherences during the evolution period. In this context, it should be mentioned that there are MP sequences for which such bracketing pulses are unnecessary, since the evolving coherences and the effective field are automatically perpendicular to each other during the whole sequence (*36, 37*). The adaptation of such sequences to fast MAS conditions might be feasible and promises further improvement of the resolution.

In the MQ experiment, following the evolution period, the MQ coherences are reconverted back to detectable SQ coherences, while the desired order of MQ coherences is selected by the conventional phase cycling techniques (*1, 2*). During the detection period, the SQ coherences can be acquired, narrowing the resonance lines by MAS alone or by simultaneous MP decoupling. For direct detection under windowless or semiwindowless MP sequences, a recently developed technique (*26*) is used in the experiments described next.

## EXPERIMENTAL AND RESULTS

The experiments were performed on L-alanine using a Bruker ASX spectrometer with a $^1$H Larmor frequency of 500 MHz. In order to provide comparable results, all experiments were carried out on a double-resonance MAS probe using rotors of an outer diameter of 2.5 mm. This equipment enables MAS spinning frequencies of up to 35 kHz. For MP dipolar decoupling in $t_1$, the 90° pulse length was set equal to 1.6 $\mu$s, resulting in a WHH-4 cycle time of $t_c = 9.6$ $\mu$s, which was synchronized with the rotor frequency ($\omega_R/2\pi = 13$ kHz corresponding to $\tau_R = 8 \cdot t_c$). For the direct detection of the SQ coherences, the WHH-4 cycles were applied asynchronously to the rotor period ($t_c = 16$ $\mu$s; see Fig. 1d), such that MAS averages the timing imperfections originating from the direct detection of the FID during the pulse train (*26*).

### *Single-Quantum Spectra*

L-Alanine is a rigid dipolar solid with a static $^1$H resonance linewidth of about 35 kHz. Therefore, at moderate rotor frequencies, DQ coherences can be easily excited using the simple five-pulse sequence of Fig. 1b (see later discussion). On the other hand, such strong dipolar couplings severely degrade the resolution. Figure 2 presents $^1$H SQ spectra of L-alanine applying MAS at a rotor frequency of (a) $\omega_R/2\pi = 13$ kHz and

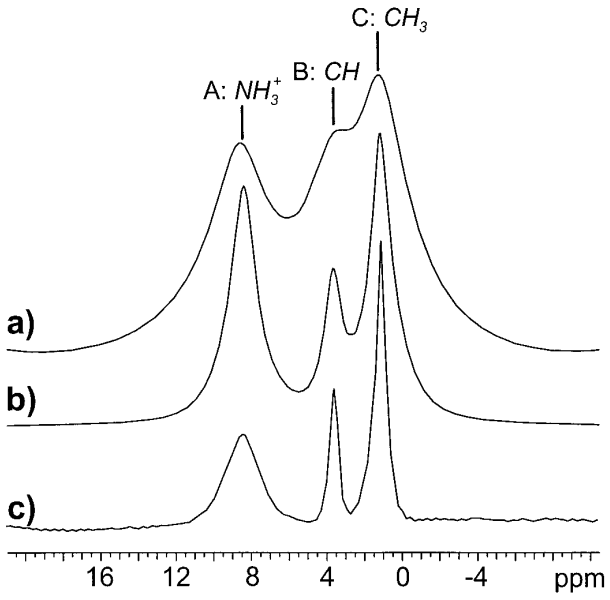


**FIG. 2.** $^1$H 500-MHz SQ spectra of L-alanine recorded using different dipolar decoupling techniques: (a) MAS at $\omega_R/2\pi = 13$ kHz. (b) Ultrafast MAS at $\omega_R/2\pi = 35$ kHz. (c) MP-assisted dipolar decoupling under MAS at $\omega_R/2\pi = 13$ kHz, using the WHH-4 sequence with direct detection (*26*) (cf. Fig. 1d). The WHH-4 sequence scales the chemical shift axis by a factor of about 0.6, which has been corrected for.

(b) $\omega_R/2\pi = 35$ kHz. As expected, the resolution is considerably enhanced by increasing the MAS spinning frequency from 13 to 35 kHz. However, even at a spinning frequency of 35 kHz, not all lines are resolved to the baseline. Only the simultaneous application of the semiwindowless WHH-4 MP sequence and MAS at $\omega_R/2\pi = 13$ kHz yields three completely resolved resonance lines (see Fig. 2c). This increase in resolution takes place despite of the chemical shift axis being scaled by a factor of, experimentally, 0.6, which agrees well with the theoretical value for WHH-4.

The decoupling efficiency of MP-assisted MAS and ultrafast MAS, however, depends on the considered resonance line. The aliphatic $^1$H resonances are narrowed by MP-assisted MAS at $\omega_R/2\pi = 13$ kHz to linewidths of about 300 Hz, whereas MAS alone at $\omega_R/2\pi = 35$ kHz still leads to linewidths of about 750 Hz. On the other hand, the resonance line of the $NH_3^+$ protons is narrowed by both decoupling techniques to about the same extent, resulting in a linewidth of about 1 kHz. Obviously, in the latter case, the $^1$H resonances are additionally broadened by $^1$H–$^{14}$N interactions, and the MP-assisted technique provides no advantage compared to pure MAS.

### *Double-Quantum Spectra under Combined Multiple-Pulse and MAS Dipolar Decoupling*

Figure 3 presents 2D $^1$H DQ spectra of L-alanine recorded under MAS at $\omega_R/2\pi = 13$ kHz with and without additional MP decoupling during the corresponding evolution periods (see Fig. 1a). In general, a DQ MAS spectrum consists of several spinning sidebands, the pattern of which has already been described elsewhere (*3, 4, 8, 14*). In order to derive qualitatively dipolar connectivities from a 2D DQ spectrum, one usually concentrates on the subspectrum at the first-order MQ spinning sideband. A quantitative consideration of DQ intensities requires either the interpretation of the complete MQ MAS sideband pattern (*4, 8, 14*) or, alternatively, the integration of all sidebands (*9*) which can be experimentally achieved by stroboscopic signal acquisition in intervals of $\Delta t_{1,2} = \tau_R$.

In the following, we consider the 2D DQ subspectrum present at the first-order DQ spinning sideband. The resonance lines are narrowed by the following four combinations of dipolar decoupling techniques: first, MAS alone at $\omega_R/2\pi = 13$ kHz (Fig. 3a); MP-assisted MAS in only one of the spectral dimensions, that is, second, $t_2$ (Fig. 3b) and, third, $t_1$ (Fig. 3c); and, fourth, MP-assisted MAS in both dimensions (Fig. 3d). It is important to note that, in the case of badly resolved peaks, the assignment is based on the *a priori* knowledge of DQ signals and the corresponding dipolar connectivities from a well-resolved 2D DQ spectrum of L-alanine (as obtained by ultrafast MAS; see later discussion).

As long as solely MAS at $\omega_R/2\pi = 13$ kHz is applied, the two aliphatic $^1$H resonances are not separated, and the DQ peaks can hardly be assigned (see Fig. 3a). For L-alanine, three diagonal peaks (AA, BB, CC) and three cross-peaks (AB, AC, BC) are expected, owing to dipolar connectivities between the $NH_3^+$ (A), CH (B) and $CH_3$ (C) protons, respectively.

Application of a WHH-4 pulse sequence in addition to MAS during the detection period $t_2$ enhances the resolution in the SQ dimension and separates all three resonances completely (see Fig. 3b). As known from the WHH-4 decoupled SQ spectrum in Fig. 2c, the $NH_3^+$ proton resonance line is broader and less intense compared to the aliphatic resonances. However, the different DQ peaks are still not resolved in the DQ dimension.

In Fig. 3c, MP dipolar decoupling in $t_1$ improves the resolution in the DQ dimension with $t_1$ being incremented in steps of the WHH-4 cycle time ($t_c = \tau_R/8 = 9.6$ $\mu$s). Although the resolution in the SQ dimension is provided by MAS alone at $\omega_R/2\pi = 13$ kHz, all expected DQ signals can be, at least, identified and assigned to dipolar connectivities of L-alanine. However, the improvement in resolution is accompanied by a considerable loss of signal intensity, especially for the $NH_3^+$ proton resonance, and artificial peaks are present in the spectrum. Moreover, the overall spinning sideband pattern of the DQ spectrum (not shown) is also modified by the MP sequence and, thus, cannot be interpreted in the same way as known from MAS-only spectra (*4, 8, 14*).

Up to this point, WHH-4 dipolar decoupling has been applied in the two spectral dimensions separately. Application of MP-assisted MAS in both dimensions results in the 2D DQ spectrum presented in Fig. 3d, in which most of the peaks are fully separated. It is clear that, compared to the MAS-only spectrum of Fig. 3a, MP-assisted MAS *drastically* enhances the spectral resolution in both dimensions of a DQ spectrum,

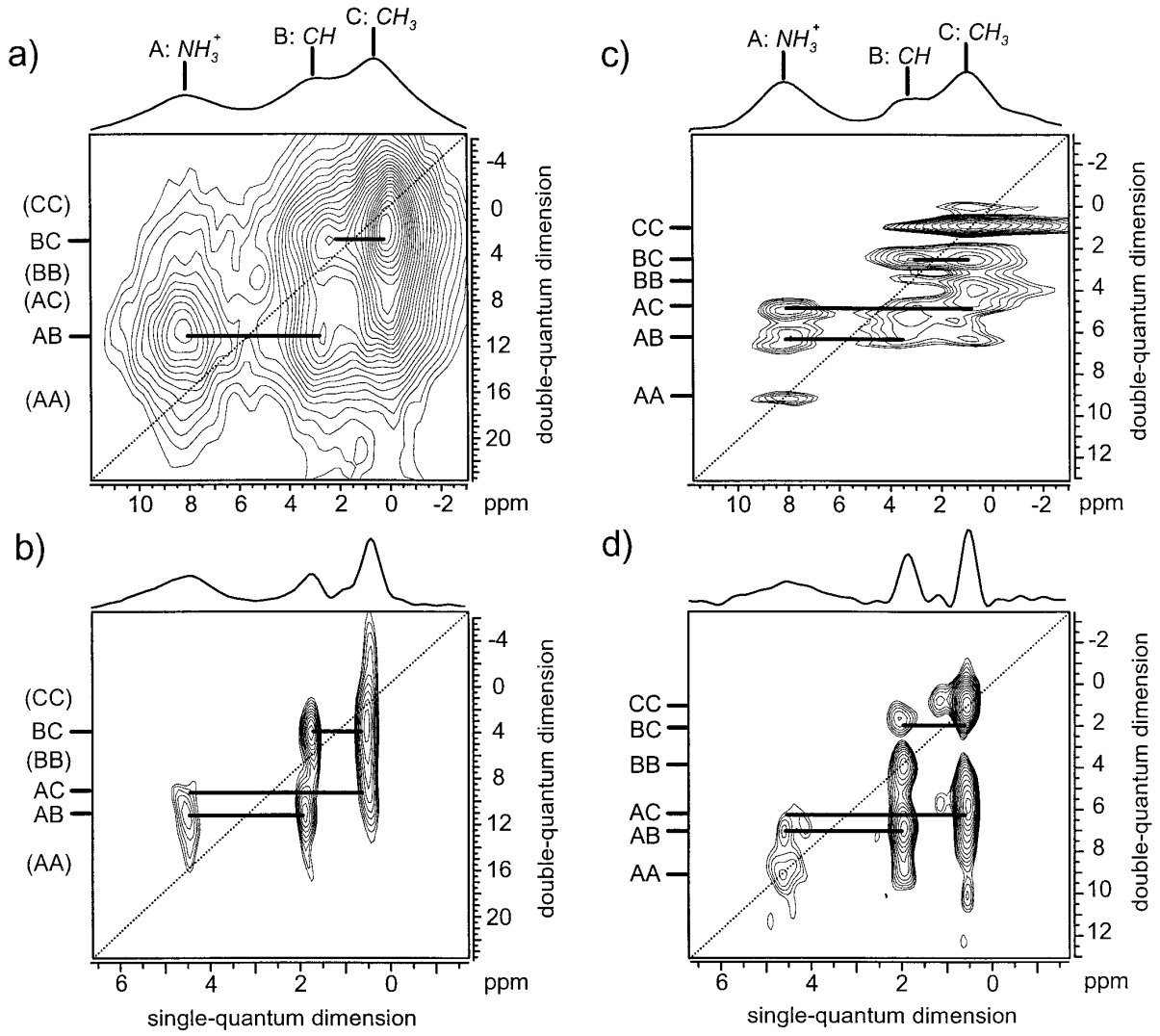


**FIG. 3.** Two-dimensional $^1$H 500-MHz DQ spectra of L-alanine using either MAS only or MP-assisted MAS for dipolar decoupling. In all cases, the spinning frequency was set equal to 13 kHz, and the DQ coherences were excited using the five-pulse sequence of Fig. 1b. (a) MAS alone. (b) Additional MP decoupling in the SQ dimension, (c) in the DQ dimension, and (d) in both dimensions. For MP decoupling, the chemical-shift axes are not corrected, so that the scaling factor of 0.6 is directly visible in the respective spectral dimensions.

although there are some minor drawbacks that still ask for further improvements.

Obviously, the MP dipolar decoupling is still more effective for SQ coherences than for DQ coherences, as can be seen from comparing the linewidths in both dimensions. There are several explanations for this difference in the line-narrowing efficiencies: First, *N*-quantum coherences are *N*-fold sensitive to any error of the pulse phases or the flip angles during the MP sequence. Second, there could be a loss of coherence order due to imperfect adjustment of the bracketing pulses. Third, as has recently been shown (*8*), MQ coherences are, in general, more sensitive to additional spin interactions and, in particular, to dipolar line-broadening effects than are SQ coherences.

In addition to the different decoupling efficiencies in both dimensions, there are weak artificial peaks present in the spectrum. These signals result from the well-known sensitivity of MP decoupling techniques to any kind of experimental misadjustments. In the case of MQ coherences, this sensitivity is even magnified for the same reasons outlined in the previous discussion of the MP dipolar decoupling efficiency. In order to avoid any undesired perturbation of the MQ evolution, a precise adjustment of all experimental parameters is required.

Apart from that, for both DQ spectra with MP decoupling in $t_1$ (Figs. 3c and 3d), the signal intensity and the effective line narrowing of the $NH_3^+$ proton resonances are to be improved. This feature of MP decoupled spectra has already been observed for the SQ spectrum (cf. Fig. 2). Nevertheless, the main objective of this section is clearly achieved. The principal strategy which makes resolution enhancement by MP decoupling sequences applicable to both dimensions

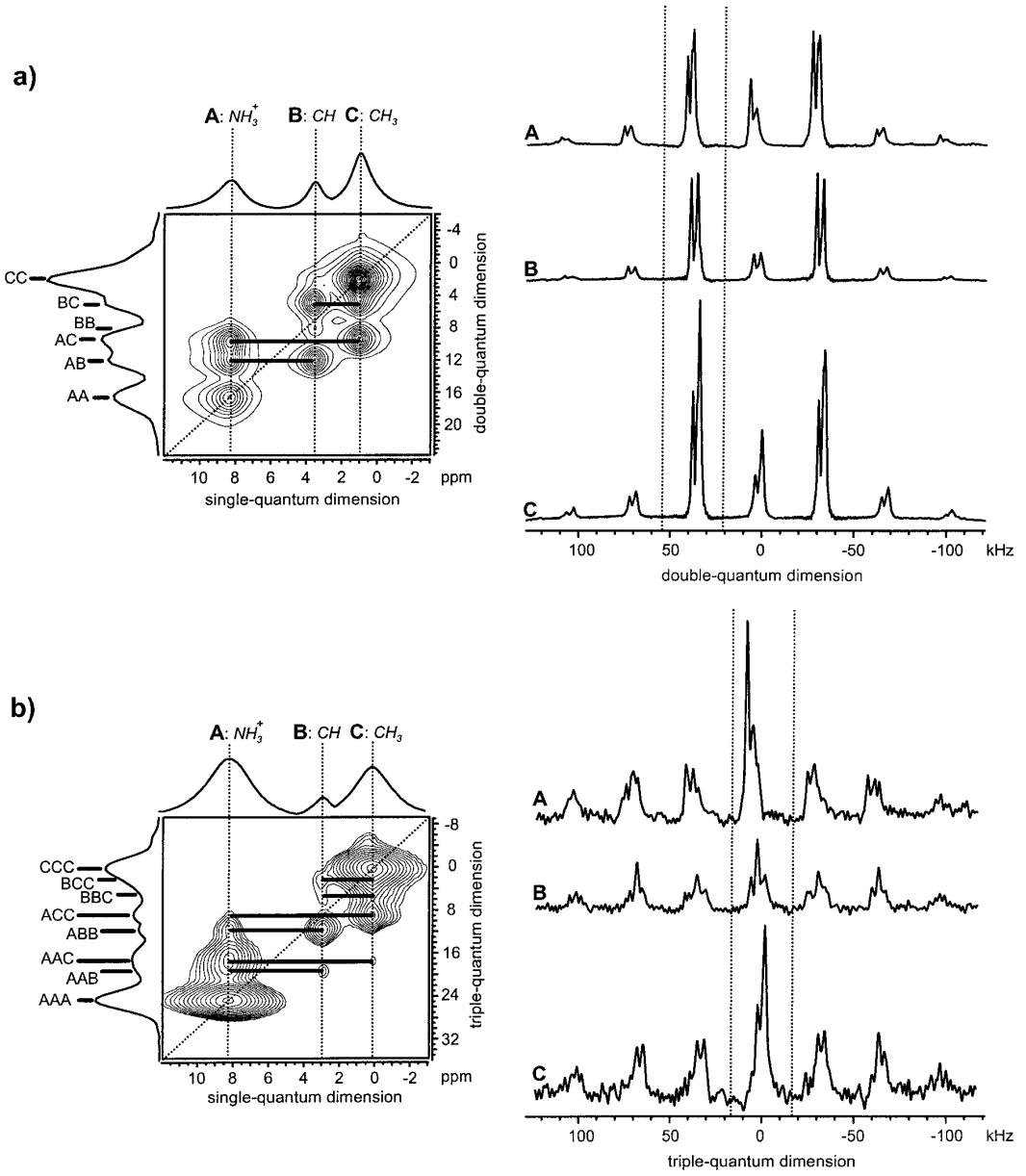


**FIG. 4.** Two-dimensional MQ $^1$H 500-MHz spectra of L-alanine recorded under MAS at $\omega_R/2\pi$ = 35 kHz, applying the BABA recoupling pulse-sequence of Fig. 1c. (a) DQ spectrum with $\tau_{exc} = \tau_R$, and (b) TQ spectrum with $\tau_{exc} = 2\tau_R$. On the left, the subspectra at the first-order DQ sideband and the TQ centerband, respectively, are shown, as indicated by the marked regions of the slices on the right. From these 2D subspectra, dipolar connectivities between pairs (DQ) or triads (TQ) of protons can be directly determined. On the right, slices at each of the three $^1$H SQ resonances show the typical MQ spinning-sideband patterns.

of the MQ MAS experiment is introduced and experimentally demonstrated.

*Multiple-Quantum Spectra under Ultrafast MAS*

After considering the dipolar decoupling performance of the WHH-4 sequence combined with MAS at $\omega_R/2\pi$ = 13 kHz, we now give examples of 2D MQ spectra recorded under ultrafast MAS. At spinning frequencies of $\omega_R/2\pi$ = 35 kHz, the condition for the fast MAS regime, that is, $\omega_R > \omega_d$ (where $\omega_d$ is the strength of the static dipolar interaction), is fulfilled, in almost all cases, for dipolar couplings between pairs of protons. Hence, the five-pulse sequence used at moderate spinning frequencies, that is, $\omega_R/2\pi \leq 15$ kHz, has to be replaced by a recoupling pulse sequence such as BABA (*10*, *14*).

The 2D DQ spectrum of L-alanine obtained using MAS-only decoupling with $\omega_R/2\pi$ = 35 kHz and an excitation period of $\tau_{exc} = \tau_R$ = 28.6 $\mu$s is given in Fig. 4a. Compared to the MAS-only spectrum with $\omega_R/2\pi$ = 13 kHz in Fig. 3a, the most striking feature is the drastic increase of spectral resolution. All DQ resonances can be precisely identified and, thus, the dipolar

connectivities in L-alanine can be determined from the 2D DQ spectrum. As a specific example, consider the connectivity of the C–H proton (B) in Fig. 4a. It exhibits strong couplings to the other protons at distances of about 0.24 nm, but virtually no intermolecular coupling to its equivalent at a distance of 0.36 nm (*38*).

Compared to the MP decoupled spectrum given in Fig. 3d, it can be clearly seen that, although the MP technique provides a slightly better resolution, at the current state of development, it does not measure up to the standard of quality of MQ MAS spectra provided by ultrafast MAS.

In contrast to the DQ spectra with MP decoupling in $t_1$ (Figs. 3c and 3d), the characteristic DQ spinning-sideband pattern can be obtained, for all six DQ coherences, directly from the 35-kHz DQ MAS spectrum by extracting slices in the DQ dimension at the three different SQ resonances. The existence of those spinning-sideband patterns (with relatively high intensities up to the third order) shows that the overall dipolar couplings in L-alanine are still comparable to the spinning frequency even at a value of $\omega_R/2\pi = 35$ kHz which agrees with static linewidth. Thus, structural information on dipolar coupling strengths (*4, 14*) and the spin topology (*8*) is still accessible under ultrafast MAS conditions, as we shall briefly outline in the following.

In the fast MAS regime, an isolated pair of spin-$\frac{1}{2}$ nuclei leads to symmetric DQ signals at odd-order spinning sidebands only (*14*). For $\omega_R \gg \omega_d$, the signal intensity is concentrated in the first-order sidebands. As is evident from Fig. 4a, all coherences in L-alanine also show spinning sidebands for even-order multiples of the rotor frequency. This indicates the influence of spins surrounding the considered spin pair. Nevertheless, the spectrum is dominated by its first-order spinning sidebands even for the AA and CC coherences, although they originate from protons which are part of the three-spin systems $NH_3^+$ (A) and $CH_3$ (C). At moderate MAS frequencies, those three-spin topologies lead to DQ spectra with a dominating centerband. At spinning frequencies of 35 kHz, however, the dipolar decoupling suffices to emphasize the pair character even among $NH_3^+$ and $CH_3$ protons. The fact that the AA and CC resonances show the most intense peaks in the central region of the DQ spinning sideband pattern exhibits the residual influence of the third spin in the $NH_3^+$ and $CH_3$ groups.

The $^1$H triple-quantum (TQ) spectrum of L-alanine presented in Fig. 4b was also obtained under MAS at $\omega_R/2\pi = 35$ kHz. For TQ excitation, the BABA recoupling sequence (Fig. 1c), extended by bracketing pulses to prepare an initial state $\rho(0) \propto I_{x,y}$, was applied with $\tau_{exc} = 2\tau_R = 57$ $\mu$s. As described previously for the DQ spectrum, ultrafast MAS combines for 2D TQ spectra as well a drastic increase in spectral resolution with an artifact-free quality of signal. Although, with increasing order of MQ coherences, the signal is less intense and there are more peaks present in the 2D spectrum, TQ coherences among all possible proton triads could be excited and identified in the 2D TQ spectrum (AAA, AAB, AAC, ABB, ACC, BBC, BCC, and CCC). As expected, the TQ coherences involving only either $NH_3^+$ or $CH_3$ protons, that is, AAA and CCC, lead to the most intense peaks.

It should be noted that not all TQ resonance lines are clearly resolved in the TQ dimension, and that most of the cross-peaks are considerably asymmetric. The latter feature is, to a certain extent, inherent to TQ coherences. An AAB TQ coherence, for example, splits into two peaks in the SQ dimension, located at the respective resonance frequencies of A and B. The ratio of signal intensities A:B is then expected to be equal to 2:1. The observed asymmetry is, however, much stronger than that, because, at the end of the reconversion period, after the AAB TQ signal has been split into its A and B part, the relaxation behavior and hence the linewidth are different for the two parts (*8*).

In addition to the connectivities derived from the 2D TQ spectrum, the TQ spinning-sideband pattern contains, analogously to DQ spectra, further information on the spin topologies. The origin of these TQ MAS patterns and their content of information are discussed in detail in Ref. (*8*).

## DISCUSSION

The enhancement of resolution and sensitivity in $^1$H solid-state MQ MAS spectroscopy by ultrafast MAS or by a combination of MP decoupling and MAS at moderate spinning frequencies was demonstrated. The application of MAS at $\omega_R/2\pi = 35$ kHz results, for rigid dipolar solids, in a resolution enhancement of about a factor of 2, compared with moderate spinning frequencies of $\omega_R/2\pi \leq 15$ kHz. Since, at present, the resolution achievable by fast MAS has reached a regime where, even in rigid solids, the $^1$H chemical shifts of important groups start to be resolved, even a comparatively modest improvement in resolution actually allows MQ MAS methods to be extended to a considerable number of organic materials, which have been inaccessible up to now.

Alternatively, at moderately fast MAS frequencies, the resolution of MQ MAS spectra can be improved, even selectively in one of the two spectral dimensions, by MP decoupling. As a first example, a semiwindowless WHH-4 sequence was applied, but other decoupling pulse sequences can also be adapted for use in MQ experiments. Apart from alternative MP sequences, the Lee–Goldburg dipolar-decoupling method (*39, 40*) seems to be a promising approach. Like the WHH-4 sequence, it offers a short cycle time and the highest value of the chemical-shift scaling factor. The tilt angle of the bracketing pulses is, in this case, again $\theta_m = 54.7°$.

Both techniques, MP-assisted MAS as well as ultrafast MAS, allow high-resolution MQ spectra to be obtained. The ultrafast MAS technique additionally provides undistorted spinning sideband patterns which reflect the topologies of the strongly dipolar-coupled system. At such spinning frequencies, the MQ MAS patterns result mainly from the rotor encoding of the dipolar Hamiltonian during the reconversion period (*5, 14, 41*), while contributions from the evolution of the MQ coherences are, by MAS, suppressed to a large extent (*41*). From

such simplified patterns, information on the structure and the dynamics of the spin system can be extracted more easily.

With respect to routine applications, the experimental advantages and disadvantages of both decoupling techniques have to be considered. The acquisition of MQ spectra under ultrafast MAS is not only the far less sophisticated technique, but the resulting spectra are also artifact-free and the signal intensity is higher compared to the MP decoupling technique. Additionally, experimental MP imperfections amplify the $t_1$ noise. On the other hand, if the resolution achievable by ultrafast MAS is not sufficient, there is no alternative to the application of MP decoupling sequences. Moreover, MP decoupling can be applied selectively in certain periods, whereas MAS is present throughout the experiment.

However, the technical difficulties related with MP techniques should not be underestimated. Special attention has to be paid on the setup procedure, since MP decoupling is known to be enormously sensitive to misadjustments. Moreover, the cycle time $t_c$ of the MP sequence limits the sampling time $\Delta t \geq t_c$ and thus the spectral width in the MP decoupled spectral dimension. Therefore, the MP performance and the quality of the resulting spectra strongly depend on various experimental parameters, whereas MAS at $\omega_R/2\pi > 15$ kHz is straightforwardly applicable.

Apart from the homonuclear case discussed in this paper, heteronuclear MQ experiments in solids will particularly benefit from the use of MP sequences for dipolar decoupling. Since the experiments can be performed at moderate spinning frequencies, larger sample volumes are accessible. For experiments limited mainly by the *S*/*N* ratio, this could turn out to be an essential advantage.

## ACKNOWLEDGMENTS

The authors acknowledge financial support from the Volkswagen-Stiftung and from the Deutsche Forschungsgemeinschaft (SFB 262).

## REFERENCES

1. R. R. Ernst, G. Bodenhausen, and A. Wokaun, ''Principles of Nuclear Magnetic Resonance in One and Two Dimensions,'' Clarendon, Oxford (1987).
2. M. Munowitz and A. Pines, *Adv. Chem. Phys.* **66,** 1 (1987).
3. H. Geen, J. J. Titman, J. Gottwald, and H. W. Spiess, *Chem. Phys. Lett.* **227,** 79 (1994).
4. J. Gottwald, D. E. Demco, R. Graf, and H. W. Spiess, *Chem. Phys. Lett.* **243,** 314 (1995).
5. S. Ding and C. A. McDowell, *J. Magn. Reson. A* **120,** 261 (1996).
6. H. W. Spiess, *Ann. Rep. NMR Spectrosc.* **34,** 1 (1997).
7. S. Hafner and H. W. Spiess, *Concepts Magn. Reson.* **10,** 99 (1998).
8. U. Friedrich, I. Schnell, D. E. Demco, and H. W. Spiess, *Chem. Phys. Lett.* **285,** 49 (1998).
9. R. Graf, A. Heuer, and H. W. Spiess, submitted.
10. M. Feike, D. E. Demco, J. Gottwald, S. Hafner, and H. W. Spiess, *J. Magn. Reson. A* **122,** 214 (1996).
11. M. Feike, R. Graf, I. Schnell, C. Jäger, and H. W. Spiess, *J. Am. Chem. Soc.* **118,** 9631 (1996).
12. H. Geen, J. Gottwald, R. Graf, I. Schnell, H. W. Spiess, and J. J. Titman, *J. Magn. Reson.* **125,** 224 (1997).
13. M. Feike, C. Jäger, and H. W. Spiess, *J. Non-Cryst. Solids* **223,** 200 (1998).
14. R. Graf, D. E. Demco, J. Gottwald, S. Hafner, and H. W. Spiess, *J. Chem. Phys.* **106,** 885 (1997).
15. W. Sommer, J. Gottwald, D. E. Demco, and H. W. Spiess, *J. Magn. Reson. A* **112,** 131 (1995).
16. X. Feng, Y. K. Lee, D. Sandström, M. Edén, H. Maisel, A. Sebald, and M. H. Levitt, *Chem. Phys. Lett.* **257,** 314 (1996).
17. M. Hong, J. D. Gross, and R. G. Griffin, *J. Phys. Chem.* **101,** 5869 (1997).
18. L. Frydman and J. S. Harwood, *J. Am. Chem. Soc.* **117,** 5367 (1995).
19. A. Medek, J. S. Harwood, and L. Frydman, *J. Am. Chem. Soc.* **117,** 12779 (1995).
20. C. Fernandez and J. Amoureux, *Chem. Phys. Lett.* **242,** 449 (1995).
21. G. Wu, D. Rovnyank, B. Sun, and R. G. Griffin, *Chem. Phys. Lett.* **249,** 210 (1995).
22. S. P. Brown, S. J. Heyes, and S. Wimperis, *J. Magn. Reson. A* **119,** 280 (1996).
23. M. Hanaya and R. K. Harris, *Solid State NMR* **8,** 147 (1997).
24. G. Wu, S. Kroeker, R. E. Wasylishen, and R. G. Griffin, *J. Magn. Reson.* **124,** 237 (1997).
25. S. Hafner and H. W. Spiess, *J. Magn. Reson. A* **121,** 160 (1995).
26. S. Hafner and H. W. Spiess, *Solid State NMR* **8,** 17 (1997).
27. D. E. Demco, S. Hafner, and H. W. Spiess, *J. Magn. Reson. A* **116,** 36 (1995).
28. A. Bennett, R. G. Griffin, and S. Vega, *NMR Basic Princ. Progr.* **33,** 3 (1994).
29. U. Haeberlen, ''High Resolution NMR in Solids,'' Academic Press, New York (1979).
30. M. Mehring, ''Principles of High Resolution NMR in Solids,'' Springer-Verlag, Berlin (1983).
31. A. Keller, *Adv. Magn. Reson.* **12,** 184 (1988).
32. S. F. Dec, C. E. Bronnimann, R. A. Wind, and G. E. Maciel, *J. Magn. Reson.* **82,** 454 (1989).
33. R. E. Taylor, R. G. Pembleton, L. M. Ryan, and B. C. Gerstein, *J. Chem. Phys.* **71,** 4541 (1979).
34. G. Scheler, U. Haubenreisser, and H. Rosenberger, *J. Magn. Reson.* **44,** 134 (1981).
35. D. P. Burum, *Concepts Magn. Reson.* **2,** 213 (1990).
36. W. K. Rhim, A. Pines, and J. S. Waugh, *Phys. Rev. Lett.* **25,** 218 (1970).
37. M. Hohwy, P. V. Bower, H. J. Jakobsen, and N. C. Nielsen, *Chem. Phys. Lett.* **273,** 297 (1997).
38. M. S. Lehmann, T. F. Koetzle, and W. C. Hamilton, *J. Am. Chem. Soc.* **94,** 2657 (1972).
39. A. Bielecki, A. C. Kolbert, H. J. M. de Groot, R. G. Griffin, and M. H. Levitt, *Adv. Magn. Reson.* **14,** 111 (1989).
40. M. H. Levitt, A. C. Kolbert, A. Bielecki, and D. J. Ruben, *Solid State NMR* **2,** 151 (1993).
41. U. Friedrich, I. Schnell, S. P. Brown, A. Lupulescu, D. E. Demco, and H. W. Spiess, submitted.